CONTACT ANALYSIS OF AIRCRAFT ENGINE BEARING

Mayank Dixit[1], Dushyant Dwivedi[2]

[1] Mayank Dixit, Department of Mechanical Engineering, Vikrant Institute of Technology & Management Gwalior, Madhya pradesh, India
[2] Dushyant Dwivedi, Department of Mechanical Engineering, Vikrant Institute of Technology & Management Gwalior, Madhya pradesh, India

ABSTRACT

Modern gas turbine engine bearings are subjected to higher speeds and different loads in order to operate the aircraft efficiently. These bearings will be subjected to unbalance loads during normal flight and uni-directional radial load during maneuver. The stress developed at the contact zone between the rolling element and raceways dictates the limiting load, which in turn determines the bearing life. There will be increase in friction at the contact areas between the rolling elements and the raceways, the rolling elements and the cage and in the annular gaps between the cage and the races. The lubricating oil is usually supplied to the rolling elements through the under-race lubrication method in gas turbine engines. The quantity is very small amount for lubrication whereas most of the lubricating oil is used to remove the heat generated from the bearing. Therefore, prediction of contact stress in bearing components is significant for life analysis of bearings. Computer Optimized Ball and Roller Bearing Analysis (COBRA-AHS) is a software program which has the capability to design and analysis the bearings operating at higher speeds with mechanical and thermal loading. This paper describes the methodology to predict the contact stress, temperature distribution on typical aero engine bearing with COBRA-AHS program and FEA tool i.e. ABAQUS. The scope of the work is to estimate the contact stress, temperature distribution on a typical aero engine bearing with finite element analysis program and validation of these results with analytical calculations.

Keyword: *Contact stress, SIR Bearing, COBRA-AHS.*

1. INTRODUCTION

Modern aero engine bearings are required to spin at high DN (Bore diameter*RPM) rating for better performance of the propulsion system. Rolling element bearings are typical mechanical components that operate under concentrated-contact conditions. Loads carried by rolling element bearings are transmitted through the discrete contacts between the rolling elements and the two raceways. Even under moderate bearing load, the stresses at the contact are quite high, being on the order of 1 to 4 GPa. Well-designed bearings are, however, capable of carrying an appreciable amount of load. This is attributed to the fact that contact stress increases slowly with the applied load (to one third power for point contact and one half power for line contact) and that the material is in general compression.

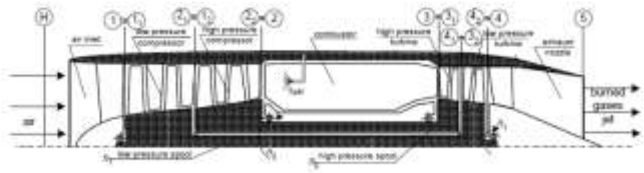

Figure 1 Schematic of Typical Gas Turbine Engine [1]

In rolling element bearings, point contact refers to the conjunction of two surfaces such that under no load, the initial contact is a single point. As load is applied, the contact develops into a finite area of a generally elliptical shape. Point contact exists between the rolling elements and raceways of ball bearings, and of roller bearings with high-crown on rollers and raceways. It also exists in roller bearings between the roller-ends and flanges. Line contact is the conjunction of two surfaces such that the initial contact under no load is a straight line. When loaded, the line spreads to form an elongated rectangle [1] The classical Hertzian theory of contact allows quick calculations of contact stress and deformation to be made from the applied load, material properties, and the internal geometry. When curved surfaces are in contact, the theoretical contact area of two spheres is a point and the theoretical contact area of two parallel cylinders is a line. As a result, the pressure between two curved surfaces should be infinite. The infinite pressure at the contact should cause immediate yielding of both surfaces. In reality, a small contact area is being created through elastic deformation, thereby limiting the stresses considerably. These contact stresses are called Hertz contact stresses. Example of curved surfaces in contact is ball bearing. Where static loads are encountered with bearings that are not rotating, resistance to plastic deformation becomes important. A limiting static capacity is commonly defined as the load corresponds to a Hertzian contact pressure of approximately 4200 N/mm^2 at the center of the contact area [2].

Deep groove ball bearing's structure is simple and is widely applied. Its main failure mode is contact fatigue spalling of rolling elements. The contact finite element analysis can show bearings' information under contact, such as contact stress, strain, penetration and sliding distance, and so on, which play a significant role in optimum design of complicated rolling bearings. Tang Zhaoping and Sun Jianping [3] studied the contact analysis for deep groove ball bearing 6200 by using ANSYS. A 3-D model of deep groove ball bearing is built by using APDL language embedded in the finite element software Ansys. Through contact analysis, the changes could be showed in stress, strain, penetration, sliding distance, friction stress among the inner ring, outer ring, rolling elements and cages. The simulation results revealed that the computational values are consistent with theoretical values. The contact analysis of finite element method can easily and intuitively get the stress and strain values as well as their cloud imagery, which can efficiently understand the parts' running information, such as contact penetration, contact sliding distance, and so on. Those will provide reference and evidence for strength analysis, life-design and structural optimum about complex bearing. B. Ramu and V.V.R. Murthy [4] studied contact analysis of cylindrical roller bearing for different roller profiles using COBRA-AHS tool. The analysis is based on two-dimensional model of roller and raceways and it found that the flat profile of roller element results in the edge stress concentration. Circular crowning eliminates the edge stress concentration at the low and moderate loads however; it develops edge concentration at heavy loads. The logarithmic profile of the roller results no edge stress concentration at low, medium and high loads and the contact stresses also distributed uniformly along the length of the roller. The optimization condition is either the maximum contact pressure at its lowest or the maximum life. Tatjana Lazovic, Mileta Reistivojevic and Radivoje Mitrovic [5] studied load distribution in rolling bearing. It found that load distribution between rolling element is unequal and degree of load distribution unequality depends on internal geometry of bearing and magnitude of external load. Two boundary load distributions in radially loaded ball bearing is defined and discussed. These are ideally equal and extremely unequal load distribution. Real load distribution is between these boundary cases. The new mathematical model of load distribution is developed respecting classic rolling bearing theory and by introduction of new, original value defined as load distribution factor. Nabhan A., Nouby M., Samy A. M. and Mousa, M. O. [6] studied contact stress distribution in deep groove ball bearing through analytical and numerical method. The contact pressure distribution between the ball and raceway of the bearing 6004 is performed by finite element software Abaqus. It found that the finite element analysis can predict contact stress in ball and raceway and The maximum stress decreases with the increase of the contact width. Furthermore, a comparison with analytical is presented. It is also concluded that the shaft misalignment leads to decrease the maximum contact stress and increase the contact area between the ball and the raceway of the bearing. Akkudasu Chennakesavulu and Amar Nageswara Rao [7] analyzed structural analysis of ball bearing using ANSYS. To analyze the stresses in a bearing system, a typical integral shaft bearing and its environment has been modelled and also investigated structural performance of integral shaft bearing to analyze its effect on bearing clearances. A comparison of a healthy integral bearing to the bearing with shaft defect and hub defect presented and results shows the equivalent stress is high for bearing with shaft defect whereas frictional stress is less, deformation is high and contact pressure is high. It observed that the bearing with shaft defect causes high damage in running conditions of the bearings. Shailendra Pipaniya and Akhilesh Lodwal [8] determined the contact stress between the inner race and ball of single row deep groove ball bearing 6210 using Hertzian contact theory and finite element analysis. The dimensional modelling has been done through modeling software Pro-e the commercial software ANSYS Workbench used as a FEA tool in this analysis work. Maximum contact stress based on Hertzian contact theory is calculated at different loads corresponding FEA is performed in order to justify the results of calculated stresses. Nagaraj k. Arakere, Nathan Branch, George Levesque and Vaughn Svendsen [9] investigated the rolling contact fatigue initiation and spall propagation characteristics of three bearing materials, namely, AISI 52100, VIM-VAR M50, and VIM-VAR M50NiL steels. Elastic and elastic-plastic subsurface stress fields are computed using finite element models that incorporate the full three-dimensional (3D) ball-raceway geometry. Elastic and elastic-plastic 3D FEA of the stress field in the neighborhood of a circular spall shows that there is extensive yielding at the spall edges due to ball rolling contact. The stress magnitudes are highest at the axial diametral locations of the spall. The combined effects of repeated impact and contact stress at the spall trailing edge resulted in material degradation, resulting in the propagation of the trailing edge in the circumferential direction.

Peng Qin and Xiaoling Zhang [10] had done the life analysis for the main bearing of aircraft engines. The 3D model of deep groove ball bearings is established by using Pro-E software and then converted into a finite element model. Secondly, such features as stiffness, strength and fatigue life of the deep groove ball bearing are investigated by ANSYS software. Based on the analysis, it found an increase of the number of rolling elements, each rolling element exposed the radial load is decrease; the contact load for each rolling element is also smaller, so fatigue life improved. An increase of the diameter of the rolling, the equivalent bearing structure increases bearing capacity increases, so the rolling element bearing life increases with the diameter increased. S. Rajendiran [11] has done metallurgical study of premium quality aircraft bearing steel (AMS 6491B). The mechanical properties of this material like yield strength / UTS, compressive strength have been tested using a computerized UTM machine. The comparative study between tensile, compressive and contact stress of this material have been carried out and discussed. The test result clearly indicates that this material possesses high level of contact stress, which is the prime requirement of high reliable bearing manufacturing.

This paper deals with the static analysis of contact stress on typical aero engine bearing using COBRA software and FEA software i.e. Abaqus. The effect of geometrical parameters such as osculation ratio, bearing clearance on Hertzian contact stress is studied. These results of contact stress are compared with that of analytical results using V

METHODOLOGY

Geometry of Ball bearing

Table 1 and Table 2, shows geometrical parameters and materials properties of ball bearing used in analysis.

Table 1, Geometric parameters of ball bearing

Ball bearing model	Spilt inner race ball bearing
Ball diameter	15.081 mm
Bore diameter	111 mm
Inner raceway diameter	87 mm
Outer raceway diameter	135 mm
Inner race groove radius	7.86 mm
Outer race groove radius	7.75 mm
Width	28 mm
No. of element	18

Table 2, Ball bearing materials

Ball bearing material	AMS 6491 M50
Modulus of elasticity	203 GPa
Poisson’s ratio	0.29
Density	7.8 gm/cm^3

Analytical Calculation

Nomenclature

α : Contact angle

v_1 & v_2 : Poisson’s ratio for the two spheres. apparent elastic modulus

σ_1 , σ_2 , σ_3 : Principle stresses

E_1 , E_2 : Young's modulus
a : Radius of the contact area
F : Acting force
Pmax : Maximum pressure
R_1 , R_2 : Radii of contact balls
Z : depth of the contact area

Hertzian Contact Stress on Ball Bearing

The Hertzian theory of elastic deformation of contact between elastic bodies can be used to find contact areas and indentation depths for simple geometries. The theoretical contact area of two spheres is shown in Fig. 1.

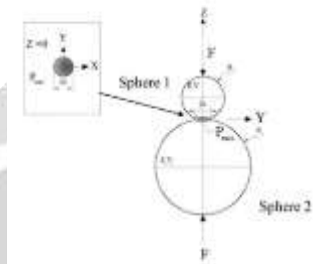

Fig. 2 Contact pressure between two spheres.

The radius of the contact area is given by:

$$a = \sqrt[3]{3F\left[\frac{1-v_1^2}{E_1}+\frac{1-v_2^2}{E_2}\right] \Big/ 4\left(\frac{1}{R_1}+\frac{1}{R_2}\right)} \quad \textbf{(1)}$$

The maximum contact pressure at the center of the circular contact area is:

$$P_{\max} = 3F \big/ 2\pi a^2 \quad \textbf{(2)}$$

The analytical model is established using setting up a program in MATLAB. The model is equipped to calculate the value of contact pressure.

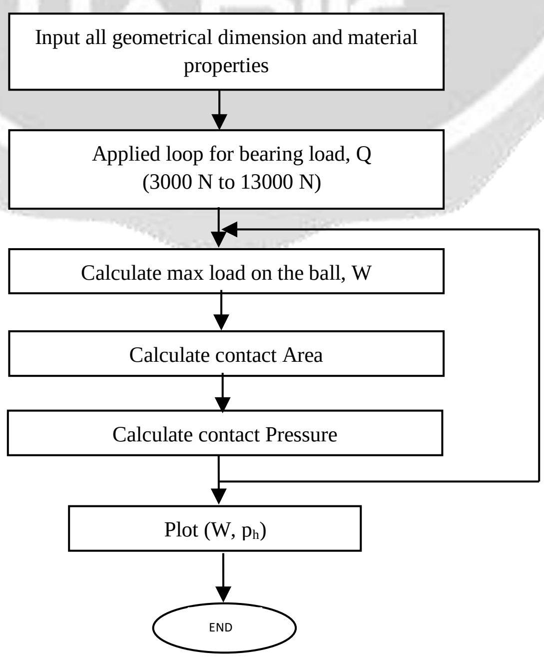

Fig 3 MATLAB flow chart

Numerical Modelling

The 3D bearing model is created through the finite element analysis tool Hyperworks. The inner and outer rings, inner and outer raceways, rolling element dimension is taken as per design. The 3D bearing is further discretized into small element for finite element analysis by using Hypermesh tool is used. The 3D model is meshed with very small element size 0.5 mm because contact analysis shows nonlinearity. For analyzing the contact in 3-D model, a coarse mesh of solid elements with fully integrated, 8-node element (C3D8) and 10-node element (C3D10M) to produce better quality for the contact surface stresses.

Fig 4 FE model of bearing

The formulation type of contact surface between the ball and races has be chosen to be penalty enforcement type with coefficient of friction of 0.01. The surface to surface contact behavior is defined in between ball and raceways because it gives more accurate results. The ball surface is considered as a master surface and raceways surface considered slave. In contact convergence master always behaves as rigid that means master surface is stiffer than surface. For controlling nonlinear static analysis, initial increment is defined 0.0 with increment 0.1.

Here the bearing radial load converted into maximum element load 'W' as the active coordinate system is cylindrical with 'x' as the axis of rotation and is applied in y-axis on all nodes of inner ring surface which is connected to RB2 rigid element. In RB2 element, one node is independent and other nodes are dependent (which follows independent node). For outer race, Outer ring of bearing is fixed in three mutual perpendicular displacement directions (U1, U2, U3); mainly x-, y- and z-direction; as well as it is non-rotational about these axis (UR1,UR2, UR3). For inner race, The inner race can be rotate with an angular velocity about its axis and the race is stationary (i.e.V1=V3=0 & VR2 = VR3 = 0). For ball, The ball is fixed in the two displacement directions (U1, U3) and as well as it is non rotational about the two axis UR2 and UR3.

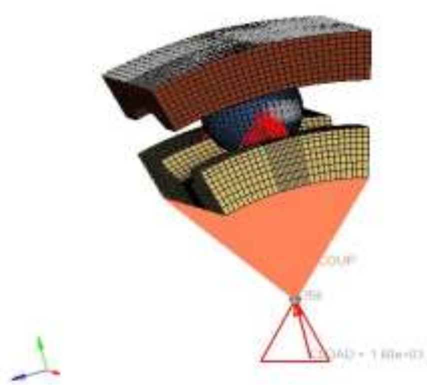

Fig 5 FE Model with load and constraints

COBRA-AHS Modelling

The bearing/shaft system model is built for COBRA-AHS analysis by using a worksheet with multiple 'tabs' to enter all input information about the bearing geometry, arrangement, operating conditions (load, speed, lubrication, temperature, etc.), materials, etc. The operating conditions of the bearing which is used in the present analysis are as listed in Table 3. The input and output sheet is generated. The structural and thermal analysis is performed on 2D model to compute the stresses, deformation and temperature distribution in ANSYS/ED which is integrated with COBRA-AHS. The output generated by COBRA-AHS includes bearing deflection due to the imposed loads, contact stresses between the elements and races, heat generation, and bearing fatigue life. The program has a modern menu-driven Windows interface, allowing users to interactively change input data and quickly see the effect on bearing performance. It also interacts automatically with the widely used ANSYS finite-element analysis program to generate finite-element models of the bearing locations. These models are used for estimating the level and distribution of temperatures within the bearing rings, balls, shaft, and housing sections, as well as temperature-induced changes in dimensions.

Table 3 Operating conditions

Inner Race speed	10000 rpm
Radial Load	10 kN
Axial Load	5 kN
Lubricant Type	MIL-L-23699
Lubricant operating temperature	80 ^{o}C
Lubricant flow rate	6.0 liters/min
Coefficient of friction	0.01

RESULTS AND DISCUSSIONS

The calculated values of contact pressure (P_{max}) should be less than allowable stress 4200 MPa for AMS 6491 M50 steel for proper functioning of ball bearing. The maximum contact pressure based on Hertz contact theory is calculated at different loads corresponding FEA is performed on Cobra-AHS and Abaqus software in order to justify the result of calculated contact pressure. The comparison of calculated contact pressure with FEA results are shown in table 4

Table 4 Max contact pressure results using Abaqus

Bearing Radial Load (N)	Max Normal Load on Element (N)	Max Contact Pressure (MPa) Analytical	Max Contact Pressure (MPa) Abaqus	Max Contact Pressure COBRA-AHS (MPa)
3000	833.3333	2566	1920	2522
4000	1111.111	2812	2359	2859
5000	1388.889	3035	2795	3085
6000	1666.667	3220	3158	3282
7000	1944.444	3401	3480	3457
8000	2222.222	3560	3707	3617
9000	2500	3690	3912	3764
10000	2777.778	3819	4112	3900
11000	3055.556	3950	4222	4027
12000	3333.333	4070	4322	4147
13000	3611.111	4183	4417	4260

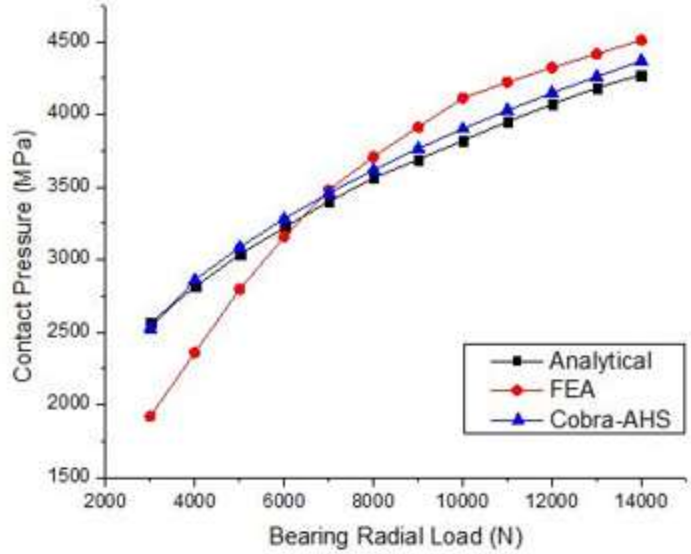

Fig 6 Effect of radial load on contact pressure

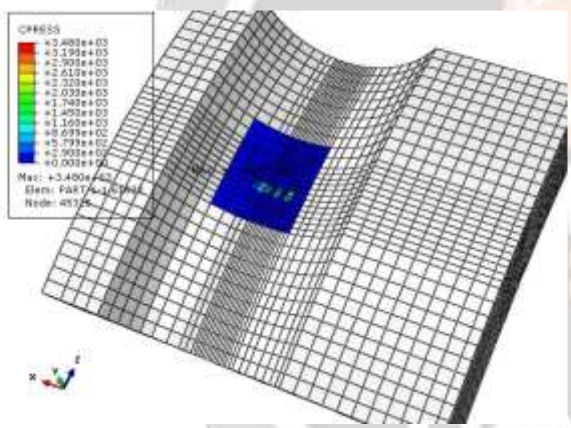

Fig 7 Contact pressure distribution inner race-ball

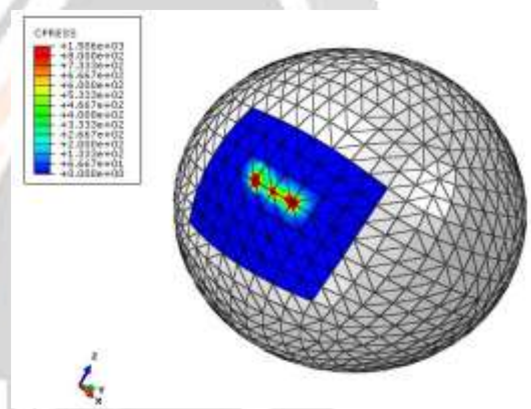

Fig 8 Contact pressure distribution in ball-outer race

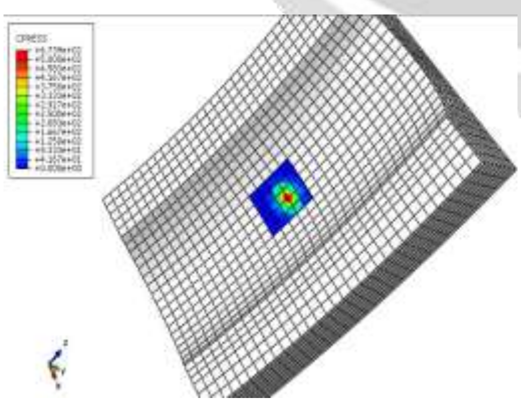

Fig 9 Contact pressure distribution in outer race - ball

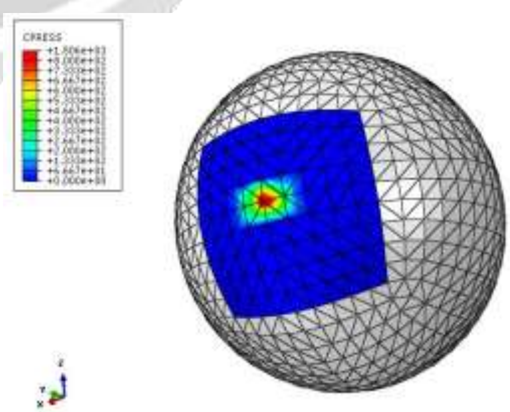

Fig 10 Contact pressure distribution in ball – inner race

It is noticed that maximum temperature shows in fig 3.15, on ball and also the von-mises stress is shows in fig 3.16, max at the contact zone between raceway and ball. The aero-engine bearings generally have stiffness 400 MN/m. So as per the design standards the split inner race bearing is worked under safe condition in present.

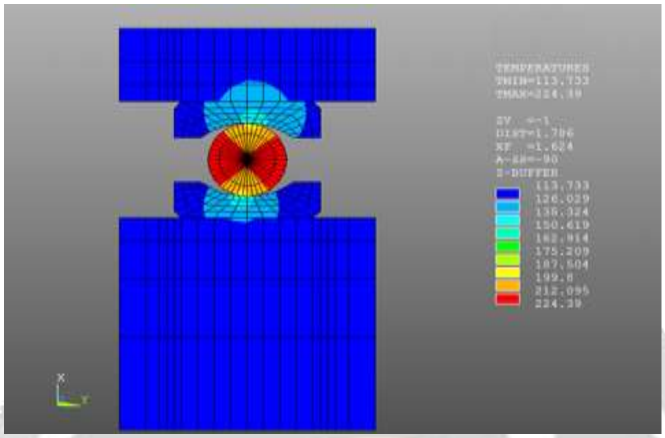

Fig 11 Temperature distribution on SIR Bearing

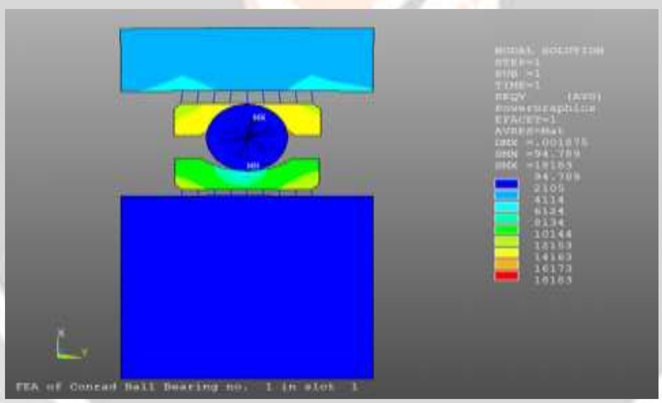

Fig 12 Von-mises stress on SIR bearing

CONCLUSION

The complete analysis of an identified aero engine bearing is performed using COBRA-AHS software and Abaqus based on Hertzian contact. Maximum Hertzian contact stresses generated for the operating load conditions are analytically calculated using contact mechanics relations using in-house developed MATLAB code. The results from the COBRA-AHS and Abaqus has good agreement with the analytical results. Contact stress distribution is plotted and discussed. The results indicate that maximum static load capacity of SIR Bearing is 14 kN. The results indicate that maximum temperature of bearing metal at 10000 rpm is around 106 C at 10 kN of radial load and 5 kN of axial loads with oil flow rate of 6 liters per minute.

REFERENCES

1. T. A. Harris, 2006, Rolling Bearing Analysis, Taylor & Francis Group, LLC.
2. Xiaolan Ai and Charles A. Moyer, 2001, Rolling Element Bearings, CRC Press.
3. Tang Zhaoping and Sun jianping, "The Contact Analysis for Deep Groove Ball Bearing Based on Ansys" International Conference on Power Electronics and Engineering Application, 1877-7058, 2011.
4. B.Ramu and V.V.V. Murthy, "The Contact Analysis of Cylindrical Roller Bearing Using Different Roller Profiles" IJRMET, vol. 3, no. 1, 2013.
5. Tatjana Lazovic, Mileta Reistivojevic and Radivoje Mitrovic, "Mathematical Model of Load Distribution in Rolling Bearing" FME Transactions, 190, vol. 36, no. 4, 2008.
6. Nabhan A., Nouby M., Samy A. M. and Mousa, M. O., "Contact Stress distribution of Deep Groove Ball Bearing Using Abaqus", Journal of the Egyptian society of Tribology, vol. 12, no.1, ISSN 2090-5882, 2015
7. Akkudasu Chennakesavulu, Amar Nageswara Rao, "Structural Analysis of Ball Bearing in ANSYS", IJSETR, vol. 04, no. 35, ISSN 2319-8885, 2015.
8. Shailendra Pipaniya, Akhilesh Lodwal, "Contact Stress Analysis of Deep Groove Ball Bearing 6210 Using Hertzian Contact Theory", International Journal of Innovative Research in Engineering & Science, vol. 7, no. 3, ISSN 2319-5665, 2014.
9. Nagaraj k. Arakere, Nathan Branch, George Levesque and Vaughn Svendsen, "Rolling Contact Fatigue Life and Spall Propagation of AISI M50, M50NiL, and AISI 52100, Part II: Stress Modeling", STLE, Tribology Transaction, 53: p. 42-51, ISSN 1040-2004, 2010
10. Peng Qin and Xiaoling Zhang, "Life Analysis for the Main bearing of Aircraft Engines," Probabilistic Safety Assessment and Management PSAM 12, June 2014, Honolulu, Hawaii.
11. S. Rajendiran, "Metallurgical study of Premium Quality Aircraft Bearing Steel (AMS 6491B)", IJMERA, vol. 1, no. 5, ISSN 2347-1719, 2013.